

Dynamical Localization and Delocalization in Polychromatically Perturbed Anderson Map

Hiroaki S. Yamada¹ and Kensuke S. Ikeda²

¹*Yamada Physics Research Laboratory, Aoyama 5-7-14-205, Niigata 950-2002, Japan*

²*College of Science and Engineering, Ritsumeikan University Noji-higashi 1-1-1, Kusatsu 525-8577, Japan*

(Dated: March 11, 2020)

In the previous paper[arXiv:1911.02189], localization and delocalization phenomena in the polychromatically perturbed Anderson map (AM) were elucidated mainly from the viewpoint of localization-delocalization transition (LDT) on the increasing of the perturbation strength ϵ . In this paper, we mainly investigate the disorder strength W -dependence of the phenomena in the AM with a characteristic disorder strength W^* . In the completely localized region the W -dependence and ϵ -dependence of the localization length show characteristic behavior similar to those reported in monochromatically perturbed case [PRE 97,012210(2018)]. Furthermore, the obtained results show that even for the increase of the W , the critical phenomena and critical exponent are found to be similar to those in the LDT caused by the increase of ϵ . We also investigate the diffusive properties of the delocalized states induced by the parameters.

PACS numbers: 05.45.Mt, 71.23.An, 72.20.Ee

I. INTRODUCTION

In recent years, localization of wave packet in quantum map systems has been extensively studied experimentally [1, 2] and theoretically [3–6]. Experimentally, Chabe *et al.* observed the critical phenomena of the localization-delocalization transition (LDT) for cold atoms in an optical lattice, which corresponds to perturbed standard map (SM). The results are interpreted based on the equivalence to Anderson transition in the three-dimensional disordered tight-binding system [7, 8].

We have proposed Anderson map (AM) that becomes the one-dimensional Anderson model in a certain limit, and investigated the parameter dependence of the LDT in the AM with the time-quasiperiodic perturbation composed of M -color modes [9, 10]. Let us define W as the disorder strength and ϵ as the perturbation strength, respectively. The characteristic ϵ -dependence and the W -dependence for the LDT in the perturbed AM were clarified in comparison with the SM under the same perturbation. A schematic representation of the resulting phase diagram for the LDT of the dichromatically perturbed AM ($M = 2$) is shown in Fig.1. The critical curve $\epsilon_c(W)$ is shown as the $\log \epsilon$ on the vertical axis and the $\log W$ on the horizontal axis.

In the previous paper [9, 10], we investigated the LDT with increasing the perturbation strength ϵ along the line L_1 or line L_4 in the Fig.1, and obtained the parameter dependence of the critical exponent of the localization length and critical strength ϵ_c by using finite-time scaling analysis of the LDT. Roughly speaking, the W -dependence of the critical curve $\epsilon_c(W)$ greatly changes around $W \simeq W^*$. Table I summarizes the difference between the time-evolution of the initially localized wave packet in $W < W^*$ and $W > W^*$ when ϵ changes along L_1 and L_4 passing the LDT points $\epsilon = \epsilon_c$.

The purpose of this paper is to give some new results

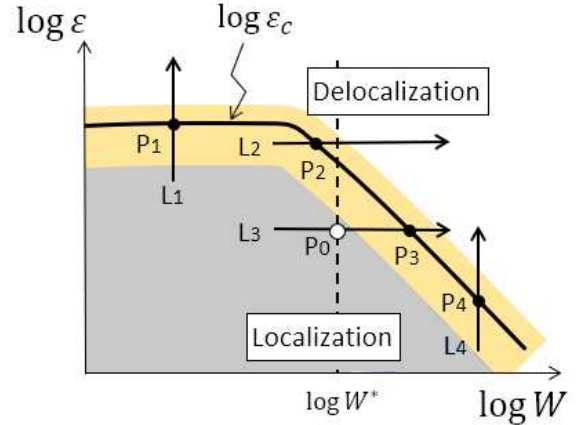


FIG. 1: (Color online) The illustrating of the critical curve $\epsilon_c(W)$ in the phase plane ($\log \epsilon, \log W$) for the dichromatically perturbed AM ($M = 2$), where $W = W^*$ is shown by dotted black line. Yellow region represents the critical region of LDT, gray represents the region where the localization length obey W^{-2} law, and light blue represents the localized region deviated from the law. Some typical paths from the localized state to the delocalized state via the LDT due to parameter changes are represented by L_n ($n = 1, 2, 3, 4$). P_n ($n = 1, 2, 3, 4$) represents the transition points in each case, and P_0 indicates the intersection with W^* when W is increased along L_3 . If the vertical axis is replaced to $\epsilon(M - 1)$, the similar phase diagram holds for the polychromatically perturbed cases ($M > 2$) [9].

and data complementary to the previous paper that have not been clearly shown yet for the localization and/or delocalization phenomena in the polychromatically perturbed AM ($M \geq 2$).

The first is the localization characteristics in the region where ϵ is small ($\epsilon < \epsilon_c$) and W is also small. In the pa-

	$\epsilon < \epsilon_c$	Ballistic	\rightarrow (Diffusive)	\rightarrow Localization
$W < W^*$	$\epsilon = \epsilon_c$	Ballistic	\rightarrow (Diffusive)	\rightarrow Subdiffusion
(L_1)	$\epsilon > \epsilon_c$	Ballistic	\rightarrow (Diffusive)	\rightarrow Diffusion
	$\epsilon < \epsilon_c$	(Ballistic)	\rightarrow Diffusive	\rightarrow Localization
$W > W^*$	$\epsilon = \epsilon_c$	(Ballistic)	\rightarrow Diffusive	\rightarrow Subdiffusion
(L_4)	$\epsilon > \epsilon_c$	(Ballistic)	\rightarrow Diffusive	\rightarrow Diffusion

TABLE I: The image of time-evolution of the spread for the initially localized wave packet in the order of the arrows. The transition from localization to diffusion is shown divided into two regions, $W < W^*$ and $W > W^*$, corresponding the Fig.6 and Fig.9, respectively. (...) represents the behavior observed in the very short time domain.

per [II], we have already investigated the W -dependence of the localization length (LL) of a monochromatically perturbed AM. As a result, the characteristics changes around $W \simeq W^*$. In this paper, we investigated changes in the LL depending on W and ϵ in the fully localized region (corresponding to the gray region in Fig.1). For both regions, $W < W^*$ and $W > W^*$, the LL shows an exponential increase with respect to ϵ , but has the parameter dependence two kinds of behavior depending on the region of the W , similar to the result already reported in Ref.[11]. When $W < W^*$, the LL shows the W^{-2} -decay, but for the region of $W > W^*$, it can be seen that the LL increases as the disorder strength W increases, regardless of the number of the modes $M(\geq 2)$.

Second, in this paper, we show characteristic behavior of this system regarding LDT when the perturbation strength ϵ is fixed, and the disorder strength W is varied along the line L_2 or line L_3 . Let the critical disorder strength W_c . In particular, in the case of $W^* < W_c$, there is a change in the localization process (transient region of time toward the localization) at $W = W^*$ before the LDT occurs at $W = W_c$, even if LDT finally occurs due to the increase of W .

Finally, we show the diffusive property of the delocalized states for $\epsilon > \epsilon_c$ and/or $W > W_c$ by using the diffusion coefficient D . The diffusion coefficient D behaves as $D \propto W^{-2}$ for $W < W^*$, and it makes minimum diffusion coefficient around $W \simeq W^*$ and it gradually increases towards a constant value for $W \gg W^*$ regardless of $M(\geq 2)$. The W -dependency for the $W \gg W^*$ region can be explained by ballistic model without localization even for the unperturbed case.

The organization of this paper is as follows. In the next section, we introduce the perturbed Anderson map with quasiperiodic modulation and the Maryland transform [12]. We show the localization property of the system in the Sect.III. The W -dependence of LDT is shown in the Sect.IV. In the Sect.V, we show the diffusive property of the delocalized states.

Also, considering the LDT along the line L1 in Fig.1, we consider the relationship between the LL in the yellow critical region and the LL in the grey region (strong localization) in appendix A. In addition, we investigated how polychromatic perturbation affects quantum states in ballistic model without localization in appendix B.

II. MODELS

The time evolution from m th step to $(m + 1)$ th step for the wave packet $|\Psi\rangle$ is described by

$$|\Psi(m+1)\rangle = \hat{U}_m |\Psi(m)\rangle. \quad (1)$$

The one-step time-evolution operator of the following Anderson map is

$$\hat{U}_m = e^{-if(m)Wv(q)/\hbar} e^{-iT(p)/\hbar}, \quad (2)$$

where $T(p) = 2 \cos(p/\hbar) = e^{-d/dq} + e^{+d/dq}$ is the kinetic energy term and $v(q) = \sum_n \delta(q-n)v_q |q| \gg |q|$ is random on-site potential. Here \hat{p} and \hat{q} are momentum and position operators, respectively. The v_n is uniformly distributed over the range $[-1, 1]$, and W denotes the disorder strength. It is a quantum map version of the Anderson model defined on the discretized lattice $q \in \mathbb{Z}$ [18]. The quasiperiodic modulation $f(t)$ is given as,

$$f(t) = \left[1 + \frac{\epsilon}{\sqrt{M}} \sum_j^M \cos(\omega_j t) \right] \quad (3)$$

where M and ϵ are number of the frequency component and the strength of the perturbation, respectively. Note that the strength of the perturbation is divided by \sqrt{M} so as to make the total power of the long-time average independent of M , i.e. $\overline{f(t)^2} = 1 + \epsilon^2/2$, and the frequencies $\{\omega_i\} (j = 1, \dots, M)$ are taken as mutually incommensurate number of $O(1)$.

We can regard the harmonic perturbation as the dynamical degrees of freedom. To show this we introduce the classically canonical action-angle operators ($\hat{J}_j = -i\hbar \frac{\partial}{\partial \phi_j}, \phi_j$) representing the harmonic perturbation as the linear modes, and we call them the ‘‘color modes’’ hereafter. We consider the Hamiltonian H_{aut} so as to include the color modes,

$$H_{aut}(\hat{p}, \hat{q}, \{\hat{J}_j\}, \{\hat{\phi}_j\}) = T(\hat{p}) + Wv(\hat{q}) \left[1 + \frac{\epsilon}{\sqrt{M}} \sum_j^M \cos \phi_j \right] \delta_t + \sum_{j=1}^M \omega_j \hat{J}_j, \quad (4)$$

where $\delta_t = \sum_{m=-\infty}^{\infty} \delta(t-m)$. One can easily check that by Maryland transform the eigenvalue problem of the

quantum map system interacting with M -color modes can be transformed into $d(= M + 1)$ -dimensional lattice problem with disorder. Let us consider an eigenvalue equation

$$e^{-i\hat{A}}e^{-i\hat{B}}e^{-i\hat{C}}|u\rangle = e^{-i\gamma}|u\rangle, \quad (5)$$

where

$$\begin{cases} \hat{A} = (Wv(\hat{q}) + \sum_j^M \omega_j \hat{J}_j)/\hbar, \\ \hat{B} = v(\hat{q})\frac{\epsilon W}{\sqrt{M}} \sum_j^M \cos \phi_j/\hbar, \\ \hat{C} = 2 \cos(\hat{p}/\hbar)/\hbar \end{cases} \quad (6)$$

for the time-evolution operator. γ and $|u\rangle$ are the quasi-eigenvalue and quasi-eigenstate. Here, if the eigenstate representation of \hat{J}_j is used, $\hat{J}_j|m_j\rangle = m_j\hbar|m_j\rangle (m_j \in \mathbb{Z})$, we can obtain the following $(M + 1)$ -dimensional tight-binding expression by the Maryland transform [9]:

$$D(n, \{m_j\})u(n, \{m_j\}) + \sum_{n', \{m'_j\}} \langle n, \{m_j\} | \hat{t}_{AM} | n', \{m'_j\} \rangle u(n', \{m'_j\}) = 0, \quad (7)$$

where $\{m_j\} = (m_1, \dots, m_M)$. Here the diagonal term is

$$D(n, \{m_j\}) = \tan \left[\frac{Wv_n + \hbar \sum_j^M m_j \omega_j}{2\hbar} - \frac{\gamma}{2} \right], \quad (8)$$

and the \hat{t}_{AM} of the off-diagonal term is

$$\hat{t}_{AM} = i \frac{e^{-i\frac{\epsilon W}{\sqrt{M}}v(\hat{q})(\sum_j^M \cos \phi_j)/\hbar} - e^{i2 \cos(\hat{p}/\hbar)/\hbar}}{e^{-i\frac{\epsilon W}{\sqrt{M}}v(\hat{q})(\sum_j^M \cos \phi_j)/\hbar} + e^{i2 \cos(\hat{p}/\hbar)/\hbar}}. \quad (9)$$

It follows that the $(M + 1)$ -dimensional tight-binding models of the AM have singularity of the on-site energy caused by tangent function and long-range hopping caused by the kick δ_i .

If the off-diagonal term does not change qualitatively, there exists $W^* = 2\pi\hbar \simeq 0.78$ where the effect of the the fluctuation width of the diagonal term is saturated for the change of the disorder strength W . It can be seen that for $W > W^*$ the diagonal fluctuation width is saturated, and the effect of the W is effective only for hopping term in the form of ϵW . Therefore, it is suggested that for $W > W^*$ the phenomenon related to the transition phenomenon can be scaled in the form of ϵW .

III. LOCALIZATION PROPERTIES IN THE POLYCHROMATICALLY PERTURBED ANDERSON MAP

We use an initial quantum state $\langle n | \Psi(t = 0) \rangle = \delta_{n, N/2}$ and monitor the spread of the wave packet by the mean square displacement (MSD),

$$m_2(t) = \langle \Psi(t) | (\hat{n} - N/2)^2 | \Psi(t) \rangle. \quad (10)$$

In the unperturbed cases ($\epsilon = 0$), it is known that the AM shows the localization in the real lattice space and the localization can be retained even when the monochromatic perturbation mode is added ($\epsilon \neq 0, M = 1$). We have reported that in the monochromatically perturbed case ($M = 1$) the W^{-2} -dependence of the localization length (LL) is stably maintained even for $\epsilon \neq 0$ and $W < W^*$, but the LL increases with increase of W for $W > W^*$ at least in the weak perturbation limit $\epsilon \ll 1$. In the case with $M \geq 2$, the LDT occurs by increasing ϵ and W . However, the localization characteristics in the polychromatically perturbed AM with small $\epsilon (< \epsilon_c)$ have not been investigated yet. The purpose of this section is to show this.

A. Localization length

We compute the LL of the dynamical localization, $\xi = \sqrt{m_2(\infty)}$ for the polychromatically perturbed cases, after numerically calculating the MSD for long-time, where $m_2(\infty)$ is numerically saturated MSD. Figure 2 shows time-dependence of the MSD for different values of the perturbation strength ϵ and the disorder strength W when $M = 2, 3$. It can be seen that the LL increases as ϵ increases when the W is fixed, and the LL for the cases when the ϵ is fixed behaves somewhat complicated because of the existence of the W^* .

The W -dependence of the LL is over-plotted in Fig.3(a) for $M = 2$ and $M = 3$. We divide the W -dependence into two regions, i.e., $W < W^*$ and $W > W^*$, to clarify their characteristics. It follows that for $W \leq W^*$, the LL shows W^{-2} -decays like the case of $M = 1$, and it increases with respect to W in the region $W > W^*$.

Figure 3(b) shows the result of the ϵ -dependence in the the perturbed AM ($M = 1, 2, 3$) for $W = 1.0 (> W^*)$. It is obvious that the LL grows exponentially as the perturbation strength ϵ increases in the all cases, i.e.,

$$\xi \sim e^{c\epsilon}, \quad (11)$$

where c is a growth rate. Furthermore, as shown in Fig.4(a),(c), the exponential growth of the LL $\xi(\epsilon)$ is also confirmed by changing the disorder strength W . Figures 4(b) and (d) shows the plots of the (a) and (c) on the horizontal axis scaled as $\epsilon \rightarrow \epsilon W$, respectively. We can see that it stands very well in one straight curve. As a result, regardless of the number of color modes M the parameter dependence of the localization length for $W > W^*$ is represented as

$$\xi \sim e^{c_1 \epsilon W}. \quad (12)$$

This form is also the same as in the monochromatically perturbed AM. It follows that the LL for $W < W^*$ behaves $\xi \sim e^{c_0 \epsilon}$ with W -independent coefficient c_0 as shown in Fig.4(c).

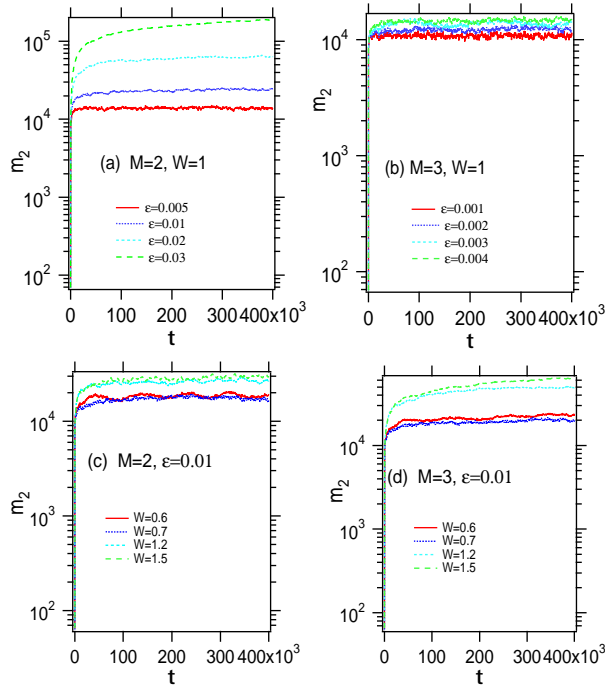


FIG. 2: (Color online) The plots of $m_2(t)$ as a function of time for different values of the ϵ and W in the polychromatically perturbed AM. (a) $M = 2$, $W = 1.0$, (b) $M = 3$, $W = 1.0$, (c) $M = 2$, $\epsilon = 0.01$ and (d) $M = 3$, $\epsilon = 0.01$. Note that the horizontal axes are in the logarithmic scale.

Therefore, if $\epsilon \ll 1$, the ϵ -dependence of the LL $\xi(\epsilon)$ of the polychromatically perturbed cases also increases exponentially as:

$$\xi(\epsilon, W) \simeq \begin{cases} cW^{-2}\exp\{c_0\epsilon\} & (W < W^*) \\ \xi_0^*\exp\{c_1W\epsilon\} & (W > W^*), \end{cases} \quad (13)$$

where the c_0 and c_1 are coefficients that increase with M .

Note that for the larger ϵ , the LL $\xi(\epsilon)$ seems to increase more strongly than the exponential function in the cases of $M \geq 2$ in Fig.3(b). This is a sign that leads to divergence at the critical point ϵ_c of the LDT. See appendix A for the more details.

B. Scaling of the dynamical localization

In this section, we recheck one-parameter scaling for the transient process to the localization. For the $W < W^*$ region and $W > W^*$ region, the different scaling property is shown.

Time-dependence of the MSD shows ballistic growth $m_2 \sim t^2$ at the initial stage of the time-evolution for $W < W^*$, and it localizes $m_2 \sim t^0$ as $t \rightarrow \infty$. Indeed, the ballistic spread of the wave packet has been observed for the short-time behavior of $m_2(t)$, as shown in Fig.6(a).

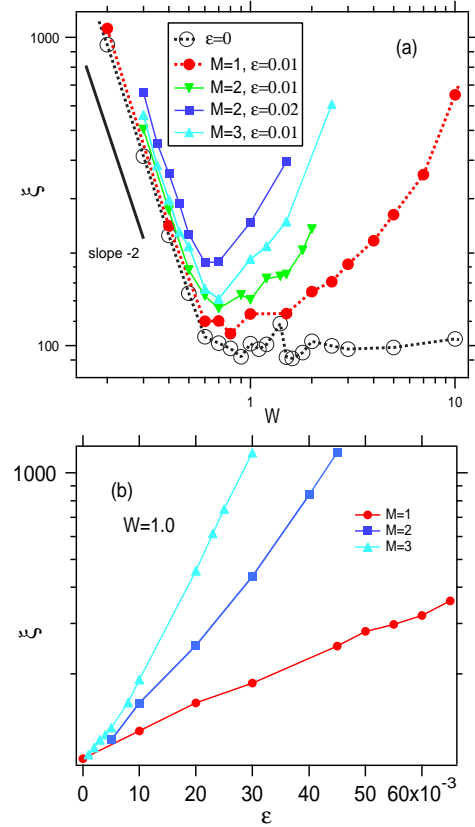


FIG. 3: (Color online) (a) Localization length of the polychromatically perturbed AM as a function of disorder strength W for various values of M and ϵ . The unperturbed case ($\epsilon = 0$) and monochromatically perturbed case ($\epsilon = 0.01$) are also plotted by the dotted line with circles and filled circles, respectively. Note that the axes are in the logarithmic scale. (b) Localization length of some perturbed AM ($M = 1, 2, 3$) as a function of ϵ with $W = 1.0$.

We use the following scaled MSD as the scaling function:

$$\Lambda(t) \equiv \frac{m_2(t)}{t^2} = F\left(\frac{t}{\xi}\right). \quad (14)$$

In this case, the fact that the localization process is scaled by the one-parameter ξ in the entire time region means the following asymptotic form of the scaling function $F(x)$:

$$F(x) \sim \begin{cases} const & x \rightarrow 0 \\ \frac{1}{x^2} & x \rightarrow \infty. \end{cases} \quad (15)$$

This type of the scaling analysis has been performed to investigate LDT phenomena at the critical point for polychromatically perturbed disordered systems [?]. The establishment of one-parameter scaling means that the asymptotic shape is smoothly connected by a single curve if the localization length is used even in the case of various parameters. Figure 5(a) shows the typical result of the

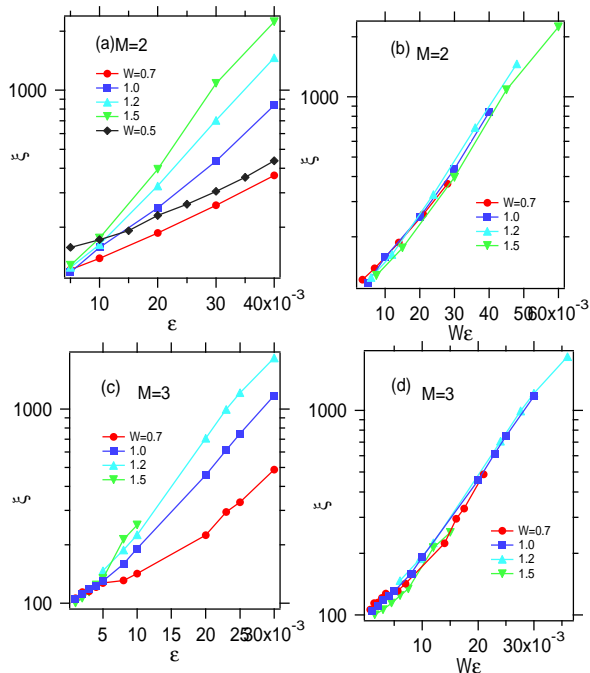


FIG. 4: (Color online) (a) Localization length ξ of the dichromatically perturbed AM ($M = 2$) as a function of perturbation strength ϵ for the relatively large W . (b) Plot of ξ as a function of ϵW for the panel (a). (c) Localization length ξ of the dichromatically perturbed AM ($M = 3$) as a function of perturbation strength ϵ . (d) Plot of ξ as a function of ϵW for the panel (c). Note that all the vertical axes are in the logarithmic scale.

localization phenomenon in (time-continuous) Anderson model by scaling the time with the localization length for various disorder strength W determined by the numerical data of MSD. It follows that the $\Lambda(t)$ roughly overlaps from the ballistic to the localized region. The horizontal axis $x = t/\xi \rightarrow \infty$ shows a decrease of the slope -2 . These results suggest that the localization process from $m_2 \sim t^2$ to $m_2 \sim t^0$ is scaled by one-parameter when the localization occurs in the system.

Let us examine the scaling for the perturbed AM. Figure 5(b) and (c) show the result of applying the same scaling to the cases with $M = 1$ and $M = 2$ with small ϵ . The localized states are obtained by changing various W s, and Λ as a function of t/ξ are displayed. Since the $x \rightarrow \infty$ side is localized, it is obvious that it is asymptotic to $\Lambda_s(x) \sim x^{-2}$. Actually, the data with varying W are also plotted, but the scaling is not bad. However, if you look closely, it follows that the scaling works well for the cases for $W < W^*$, but we can see the shift to the different curves for $W > W^*$ in the transient region to the localization. (The inset in the Fig.5(c) is an enlarged view.) In other words, this is an existence effect of W^* , and when W is increased along the line L_2 in Fig.1, these features occur at the point P_0 denoted by the white circles. In addition, as shown in the Fig.5(d), it can be seen that even for

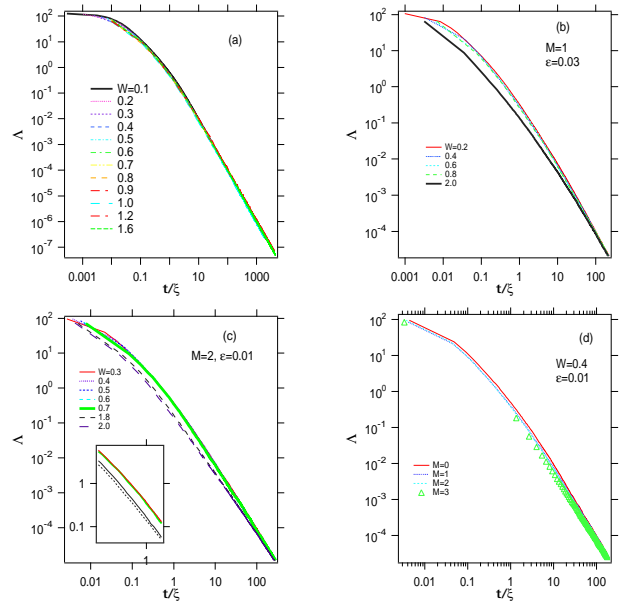


FIG. 5: (Color online) Scaled MSD $\Lambda(t)$ as a function of the scaled time $t/\xi(W, \epsilon)$, where $\xi(W, \epsilon)$ are determined by MSD for several parameter sets (M, W, ϵ) . (a) Unperturbed time-continuous Anderson model ($\epsilon = 0$) with several values of the W . (b) Monochromatically perturbed cases ($M = 1$, $\epsilon = 0.03$) with several values of the W . (c) Dichromatically perturbed cases ($M = 2$, $\epsilon = 0.03$) with several values of the W . (d) Perturbed cases ($M = 0, 1, 2, 3$) of the case with $W = 0.4$ and $\epsilon = 0.01$. Note that all axes are in logarithmic scale.

different M the similar scaling curves are obtained for the region $W < W^*$.

IV. LOCALIZATION-DELOCALIZATION TRANSITION IN THE POLYCHROMATICALLY PERTURBED AM

In the previous paper [9], we analyzed in detail LDT caused with increasing ϵ for a fixed W along Line L_1 in Fig.1. In this section, we confirm the LDT by changing the disorder strength W for the fixed ϵ along the L_2 or L_3 in the Fig.1.

A. subdiffusion of LDT

We can numerically determine the critical value ϵ_c and/or W_c of the LDT so that the MSD becomes subdiffusion,

$$m_2 \sim t^\alpha (0 < \alpha < 1). \quad (16)$$

It is known from numerical calculation that the diffusion index α is determined by the number of colors M as,

$$\alpha \simeq \frac{2}{M+1}, \quad (17)$$

regardless of the LDT produced by changing ϵ or by changing W . This is consistent with the prediction due to the one-parameter scaling (OPS).

Figures 6(a) and (b) show the $m_2(t)$ divided into two regions, $W < W^*$ and $W > W^*$, respectively, in the dichromatically perturbed AM with $\epsilon = 0.05$. This case corresponds to L_3 in the Fig. 1. In the case of $W < W^*$, the MSD increases as the W decreases, but the shape of the curve is the same and no transition to the delocalization is seen. On the other hand, in the case of $W > W^*$, the LDT occurs around $W_c \simeq 0.9$ and the MSD shows subdiffusive behavior $m_2 \sim t^{2/3}$ at the critical point. It may seem strange that the localized quantum state delocalizes as the disorder width W grows, but this is one of the features of the perturbed AM with the characteristic value $W^* (< W_c)$. Of course, it can be seen that when the W is made larger ($W \gg W_c$), the wavepacket spreads closer to the normal diffusion. We can also see how the growth of MSD changes with the value of W . In the region $W < W^*$, the ballistic increase is remarkable at the very short-time stage ($t < 10$), but in the $W > W^*$, after the ballistic growth of the short time ($t < 10$), it shows the diffusive spread after the time domain.

In Fig.7(a), in order to see the transition phenomenon along the L_3 in the case of $\epsilon = 0.05$ in which W_c is larger than W^* ($W_c > W^*$), the time-dependence of scaled MSD, $\Lambda(t, W) = \frac{m_2(t)}{t^{2/3}}$ is plotted for various W s. When W is increased the curve moves from top to bottom and rises again (denoted by green \rightarrow red \rightarrow blue) toward the LDT. In the region $W < W^*$, even if the W is increased, the MSD decreases, but there is no transition yet, and when W further increases from the $W \simeq W^*$ at the bottom, the LDT occurs at W_c . We can see the trumpet-shaped change of the scaling function $\Lambda(t)$ around the critical region $W \simeq W_c$. It should be noted that the two types of the decreasing curve (denoted by green and red lines, respectively) are different in the shape (quality). Accordingly, it follows that they cannot be overlapped in the one-parameter scaling analysis.

On the other hand, Fig.7(b) shows $m_2(t)$ along the line L_2 in the perturbed AM with $\epsilon = 0.065$ with increasing W in the case of $W_c < W^*$. The LDT occurs after the MSD decreases with the increase of W , but there is almost no trumpet-shaped lower critical region.

B. Scaling analysis of the LDT

Similar to the case of the LDT with increasing ϵ in the previous paper, here the critical exponent of the localization length can be determined by performing finite-time scaling analysis in the critical region of the LDT with changing W . This corresponds to the finite-size

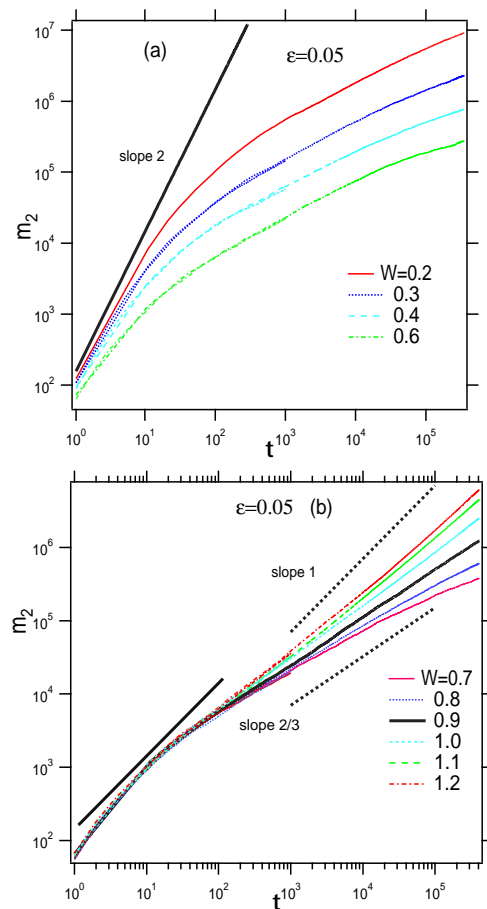


FIG. 6: (Color online) The double-logarithmic plots of $m_2(t)$ as a function of t for $M = 2$ with $\epsilon = 0.05$ including the short time region. (a) $W < W^*$, (b) $W > W^*$.

scaling analysis for Anderson transition in the higher-dimensional random system [13–16].

Figure 8 displays the results of the finite-time scaling analysis for dichromatically perturbed AM ($M = 2$) with $\epsilon = 0.05$ corresponding to Fig.6. We choose the following quantity as a scaling variable

$$\Lambda_s(W, t) = \log \left[\frac{m_2(t)}{t^\alpha} \right]. \quad (18)$$

For $W > W_c$, the $\Lambda_s(t)$ increases and the wave packet delocalizes with time. On the contrary, for $W < W_c$, $\Lambda_s(t)$ decreases with time and the wave packet turns to the localization. In the vicinity of the LDT, for $\Lambda_s(t)$, OPST is assumed with localization length $\xi_s(W)$ as the parameter. Then, $\Lambda_s(W, t)$ can be expressed as,

$$\Lambda_s(W, t) = F(x), \quad (19)$$

where

$$x = |W_c - W| t^{\alpha/2\nu}. \quad (20)$$

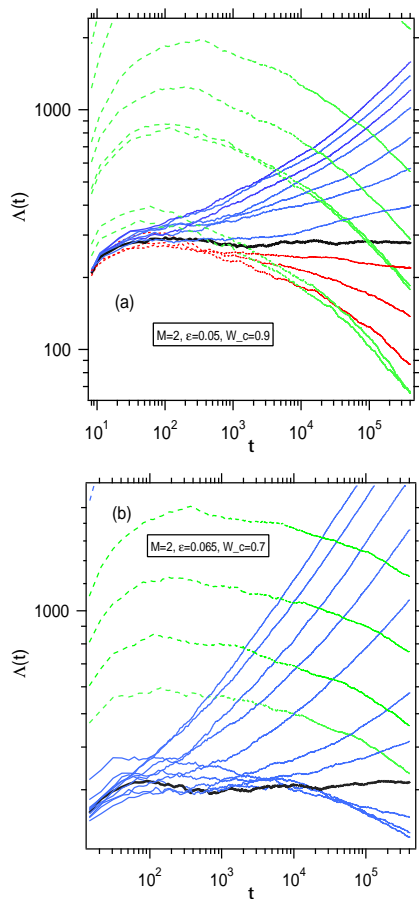


FIG. 7: (Color online) The double-logarithmic plots of scaled $\Lambda(W, t) = m_2(t)/t^{2/3}$ as a function of time in the dichromatically perturbed AM ($M = 2$). (a) The case with $\epsilon = 0.05$ for different values of the disorder strength W along the L_3 in the Fig.1, where the critical case $W_c \simeq 0.9$ is shown in by thick black line. (b) The case with $\epsilon = 0.065$, where the critical case $W_c \simeq 0.7$ is shown in by thick black line. The trumpet-shaped behavior of the $\Lambda(W, t)$ can be observed in the panel (a) because $W^* < W_c$.

$F(x)$ is a differentiable scaling function and the α is the diffusion index. Figure 8(b) shows the plot of $\Lambda_s(t)$ as a function of W at several times t , and it can be seen that this intersects at the critical point W_c . In addition, Fig.8(c) shows the plot of

$$s(t) = \frac{\Lambda_s(W, t) - \Lambda_s(W_c, t)}{|W_c - W|} \quad (21)$$

$$\propto t^{\alpha/2\nu}. \quad (22)$$

as a function of t , and the critical exponent $\nu = 1.48$ of the LDT is determined by best fitting this slope which is similar result obtained in previous paper for the LDT [9].

In Fig.8(a), we plot Λ_s as a function of $x = t^{\alpha/2}/\xi_s(W)$ for different values of W by using the obtained the critical exponent ν . It is well scaled and demonstrates the

validity of the OPS. The upper and lower curves represent the delocalized and localized branches of the scaling function, respectively. The establishment of OPS shows the equivalence of the time change and the parameter change in the $m_2(t, \epsilon, W)$.

Around the critical point of the LDT, the localization length ξ_s is supposed to diverge as

$$\xi_s \simeq \xi_0 |W_c - W|^{-\nu} \quad (23)$$

at $W = W_c$. (ξ_s depends on the number of modes M , but the subscript M is omitted.)

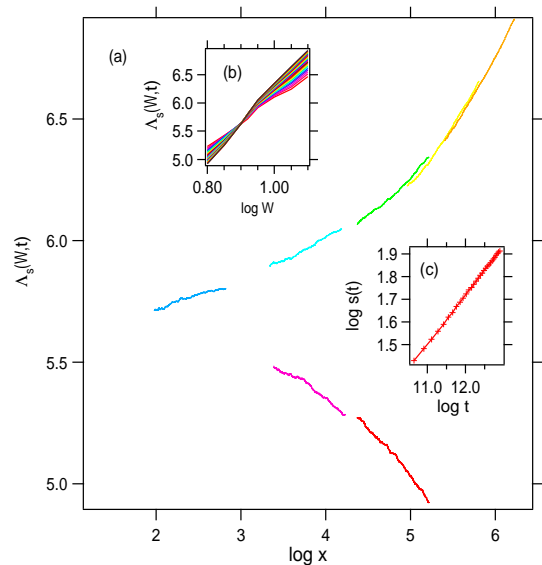


FIG. 8: (Color online) The results of the critical scaling analysis for dichromatically perturbed AM ($M = 2$) with $\epsilon = 0.05$. (a) The scaled MSD $\Lambda_s(W, t)$ with $\alpha = 0.65$ as a function of $x = \xi_0 |W_c - W|^{-\nu} t^{\alpha/2\nu}$ for some values of W . (b) The same scaled MSD $\Lambda_s(W, t)$ as a function of W for some some pick up time. The crossing point is $W_c \simeq 0.9$. (c) $s(t) = \log(\Lambda(W, t)/\Lambda(W_c, t))/(W_c - W)$ as a function of t . The critical exponent $\nu \simeq 1.48$ is determined by a scaling relation Eq.(22) by the least-square fit for data in (c).

V. DELOCALIZED STATES AND NORMAL DIFFUSION

In this section, we evaluate how the delocalized states spread due to the changes in W and $\epsilon (> \epsilon_c)$. Is this true that if $\epsilon > \epsilon_c$ the delocalized states asymptotically approach the normal diffusion as $t \rightarrow \infty$? Little is known about the models of quantum systems in which normal diffusion occurs without any stochastic fluctuation [17].

A. Delocalized states

Figure 9 shows the long-time behavior of the MSD for $\epsilon > \epsilon_c$ in the polychromatically perturbed AM ($M = 4, 6$). It seems that regardless of M the MSD approaches to the normal diffusion as $m_2 \sim t^1$ when ϵ is large. It can be expected that the normal diffusion occurs in a longer time even if ϵ is relatively small if $\epsilon > \epsilon_c$ because the scaling curve for various ϵ s neatly fit on one curve. The inset is an enlarged view in a short-time domain ($t < 10^2 (\equiv t_0)$) before the perturbation starts to work. Here, it can be seen that since $W = 2 (> W^*)$ the perturbation works after passing through the diffusive time domain ($t < t_0$).

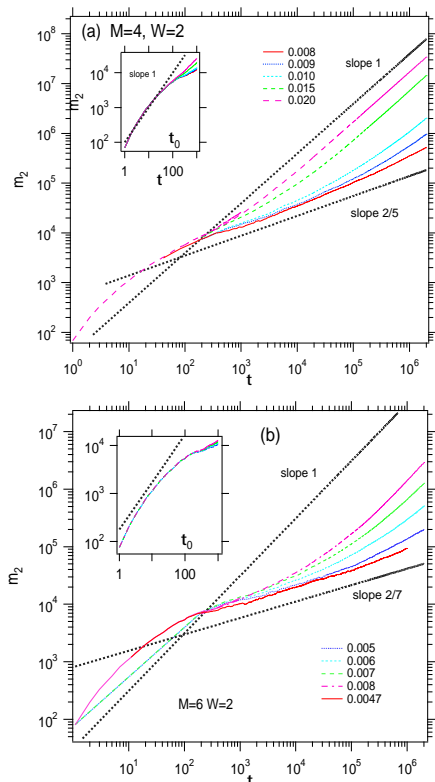


FIG. 9: (Color online) The double-logarithmic plots of $m_2(t)$ as a function of t for different values of ϵ in the polychromatically perturbed AM with $W = 2$ including the detail short time region. (a) $M = 4$ and (b) $M = 6$. The insets are the enlarged view of the short-time region $t < 10^3$.

B. W -dependence of the diffusion coefficient

As shown in the Fig.6, it can be expected that $m_2(t)$ asymptotically approaches to the normal diffusion as the $W (> W_c)$ increases for the fixed ϵ . Indeed, Fig.10 shows the time-dependence of the MSD by changing W in the case of the polychromatically perturbed AM with $\epsilon =$

$0.2 (>> \epsilon_c)$. As shown in the Fig.10(a), the $m_2(t)$ behaves the normal diffusion,

$$m_2(t) \simeq Dt, \quad (24)$$

for $M = 2$, where D is the diffusion coefficient. As shown in the Fig.10(b), similar results are confirmed even for the case of $M = 6$. Figure 11 shows the W -dependence of the diffusion coefficient numerically estimated. Regardless of the number of colors M , in the region $W \ll W^*$ it behaves

$$D \propto \frac{1}{W^2}. \quad (25)$$

However, when the W increases, it does not decrease monotonously, but it shows the minimum of D around W^* and gradually increases towards the constant value and it becomes

$$D \sim \text{const}. \quad (26)$$

for $W \gg W^*$. This behavior can be inferred from the Maryland transform as follows. For $W \simeq W^*$, the effect of the randomness of the diagonal term saturates, and the range of the random hopping term still increases even for $W > W^*$ when the $\epsilon = 0.2$. This tendency does not depend on the number of colors M after the LDT.

The above behavior of the diffusion coefficient for the weak disorder region ($W < W^*$) can be explained from the W -dependence of the localization length in the localized side. First, the W -dependence of the localization length is assumed to be $\xi(W) \propto 1/W^2$ for $W \ll 1$. As seen in the Table 1, for $\epsilon > \epsilon_c$, the MSD changes from the ballistic motion to the diffusion as the time elapses. If the duration (characteristic time) of this ballistic motion is τ , it can be estimated as

$$\tau \simeq \frac{\xi(W)}{2\pi}. \quad (27)$$

This is equivalent to considering the time evolution of the wave packet in Brownian motion, assuming that memory is lost at τ , for the weak disorder region ($W < W^*$). By using the characteristic time τ , the time-dependence of $m_2(t)$ is expressed as

$$m_2(t) \sim \xi^2 \frac{t}{\tau}, \quad (28)$$

if we consider ξ spreads every time $\tau = \xi/2\pi$. Then if the ϵ is fixed, the diffusion coefficient becomes

$$D = \lim_{t \rightarrow \infty} \frac{m_2(t)}{t} = \frac{\xi^2}{\tau} \quad (29)$$

$$\sim \frac{1}{W^2}. \quad (30)$$

As a result, the W -dependence of the localization length propagates to that of the diffusion coefficient.

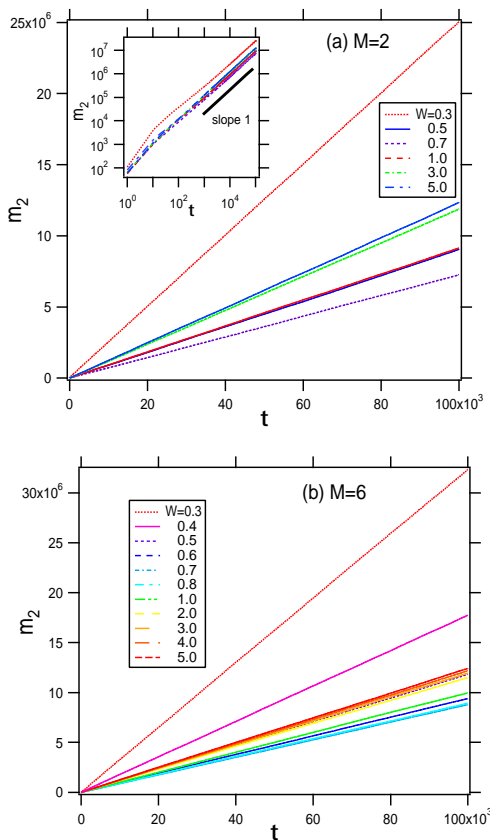


FIG. 10: (Color online) The plots of $m_2(t)$ as a function of t for different values of W in the polychromatically perturbed AM with $\epsilon = 0.2$. (a) $M = 2$ and (b) $M = 6$. Note that the axes are in the logarithmic scale. The inset of the panel (a) is in the logarithmic scale. Black dotted line shows $m_2(t) \propto t^1$ for reference.

C. ϵ -dependence of the diffusion coefficient

Next, let's examine the ϵ -dependence of the diffusion coefficient of the delocalized states. The ϵ -dependence at $\epsilon > \epsilon_c$ for $M = 2, 3$, fixed at $W = 1$, is shown in Fig.12. It can be seen that the diffusion coefficient of the delocalized state increases gradually with increasing ϵ , and saturates beyond $\epsilon \simeq 1$. This tendency also does not depend on the number of colors if the LDT occurs when $M \geq 2$. What does this value $\epsilon \simeq 1$ mean? Its meaning can be understood by replacing the time-dependent part $f(t)$ of the potential with

$$g(t) = \left[\frac{\epsilon}{\sqrt{M}} \sum_i^M \cos(\omega_i t + \theta_i) \right]. \quad (31)$$

This case can be called a ballistic model because there is no localization in the unperturbed case ($\epsilon = 0$). Actually, the ϵ -dependence of the diffusion coefficient in the ballistic model is also plotted in the Fig.12. It shows $D \propto \epsilon^{-2}$ for $\epsilon < 1$ and it gradually decreases towards a certain

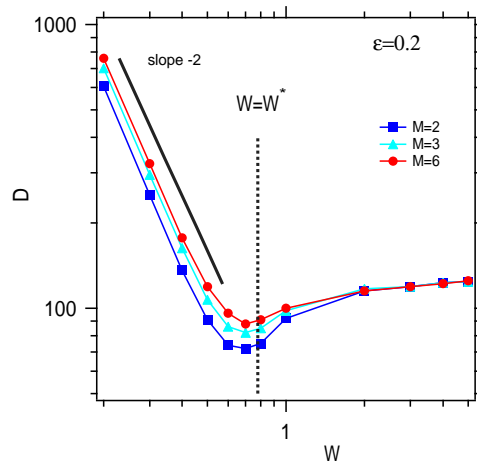


FIG. 11: (Color online) The diffusion coefficient D of the quantum diffusion as a function of W in the polychromatically perturbed AM with $\epsilon = 0.2$ of $M = 2, 3, 6$. Note that the axes are in the logarithmic scale. $D \propto W^{-2}$ and $W^* = 0.78$ are shown by black line and black dotted lines, respectively, for reference.

value when the perturbation strength ϵ increases. This is a reasonable result because the effect of the presence of "1" that gives localization at the case of $f(t)$ relatively weakens, and the time-varying term becomes more dominant. As a result, for $\epsilon \gg 1$ it can be seen that the value of the diffusion coefficient in AM is asymptotic to that in the ballistic model.

See appendix B for the details of the W -dependence of the normal diffusion in the ballistic model.

VI. SUMMARY AND DISCUSSION

We investigated the localization-delocalization transition (LDT) of the AM (Anderson map) which are dynamically perturbed by polychromatically periodic oscillations for the initially localized quantum wave packet.

The W -dependence and ϵ -dependence of the localization length (LL) in the completely localized region have characteristics similar to those of the monochromatically perturbed AM. Since the characteristic value W^* exists, the MSD shows a peculiar change with respect to the change of W , but the critical behavior of the LDT for changing W is similar to that in the LDT for changing ϵ around the critical point. In the region $W^* < W_c$, the shape of the scaling function changes, but the localization remains the same at $W = W^*$ when W increases, and the increasing W causes the LDT at a certain value $W = W_c$.

We also studied the delocalized states for $\epsilon > \epsilon_c$. The W -dependence of the diffusion coefficient of the delocalized states decreases in a form $D \propto W^{-2}$ for the region $W < W^*$. The D gradually increases towards $D \simeq const$

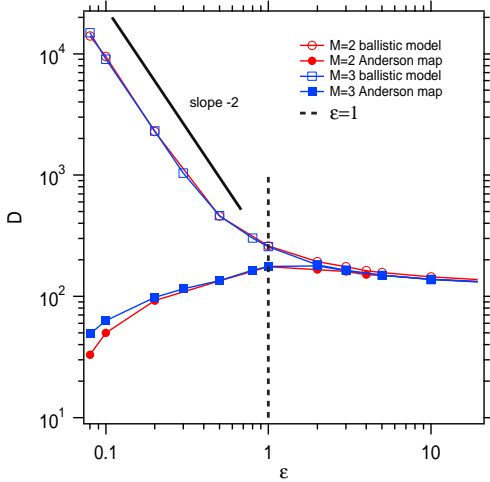


FIG. 12: (Color online) The diffusion coefficient D of the quantum diffusion as a function of ϵ in the polychromatically perturbed AM with $W = 1$ of $M = 2, 3$. The corresponding results for the ballistic model are also provided. Note that the axes are in the logarithmic scale. $D \propto \epsilon^{-2}$ and $\epsilon = 1$ are shown by black line and black dotted lines, respectively, for reference.

for $W \gg W^*$ after it becomes minimum diffusion coefficient around $W \simeq W^*$.

Roughly speaking, since the time-continuous system corresponds to $W^* \rightarrow \infty$ in the AM, it is expected that there is no LDT along the line L_2 and L_3 in Fig.1, only LDT corresponding to the region $W < W^*$ along L_1 will be observed in the time-continuous Anderson model with the time-quasiperiodic perturbation [18–20].

Appendix A: Critical phenomena of LDT and the localization length

In this appendix we consider the relation of the localization length $\xi(\epsilon)$ obtained by direct calculation for $\epsilon \ll \epsilon_c$ and the LL by finite-time scaling analysis around $\epsilon \simeq \epsilon_c$ in the polychromatically perturbed AM $W = 0.5$. We consider the LDT along the line L_1 but the same argument holds qualitatively for cases with the other parameters. The localization length $\xi_s^{(M)}(\epsilon)$ obtained indirectly from the critical scaling analysis around the critical value $\epsilon_c^{(M)}$ is expressed,

$$\xi_s^{(M)}(\epsilon) = \xi_0^{(M)} |\epsilon_c^{(M)} - \epsilon|^{-\nu^{(M)}}, \quad (\text{A1})$$

where $\xi_s^{(M)}$, $\epsilon_c^{(M)}$ and $\nu^{(M)}$ are the the localization length, critical strength and the critical exponent of the LDT, respectively. $A_0^{(M)}(W) = \xi_0(\epsilon_c^{(M)})^\nu$ can be determined by the LL of the unperturbed case $\xi_0 = \xi(\epsilon = 0)$. The order of the localization length for the different M satisfies

$$\xi_s^{(2)}(\epsilon) < \xi_s^{(3)}(\epsilon) < \xi_s^{(4)}(\epsilon) \dots \quad (\text{A2})$$

In addition, the following relations of the critical strength and critical exponent holds,

$$\epsilon_c^{(2)} > \epsilon_c^{(3)} > \epsilon_c^{(4)} > \dots, \quad (\text{A3})$$

$$\nu^{(2)} > \nu^{(3)} > \nu^{(4)} > \dots \quad (\text{A4})$$

It are established from the results and theory of the finite-time scaling analysis. In other words, considering the M -dependence of this transition, the critical value ϵ_c becomes smaller and the critical exponent ν also becomes smaller as the number of modes M increases, and the divergence of the LL around the critical value becomes mild as the M increases.

In Fig.13, we compare the localization length $\xi_s^{(M)}(\epsilon)$ decided indirectly by OPST in the critical region $\epsilon \simeq \epsilon_c$ with $\xi^{(M)}(\epsilon)$ decided directly by the saturated MSD data which are precisely calculated for ϵ 's much less than the critical region. The ϵ -dependence of these two localization lengths, $\xi_s^{(M)}(\epsilon)$, $\xi^{(M)}(\epsilon)$, seem to connect continuously, which implies unexpected wideness of the critical region in which the OPST works [21].

On the other hands, as seen in main text, even if $M = 2$ and $M = 3$, the localization length increases exponentially as ϵ increases at least for $\epsilon \ll \epsilon_c$, according to the Eq.(13). Furthermore, it seems that when ϵ increases, the localization length increases with increasing of the ϵ more strongly than the exponential growth. This is natural because ϵ grows closer to ϵ_c and leads to the divergence of the localization length at $\epsilon = \epsilon_c T$.

Appendix B: Diffusive characteristics of Ballistic model

Here we consider a model without the localization by replacing the time-dependent part $f(t)$ of Eq.(3) with $g(t)$ of Eq.(31). The system describes the free particle scattered by the quasiperiodically oscillating irregular potential. This model is also interesting as it is connected with the problem of a ballistic electrons scattered by dynamical impurities. We refer to this model as the ballistic model in this paper. The AM with the time-dependent part $f(t)$ approaches to the ballistic model in a limit $\epsilon \rightarrow \infty$, and the system has completely parameter dependence in the form of ϵW .

In the ballistic model, a simple interpretation by Maryland transform is possible. The diagonal term is a constant value that does not depend on the site. If $W = 0$ (equivalent to $M = 0$), the hopping terms are also constant, and the Hamiltonian describes the tight-binding system with periodic potential. Accordingly, the dynamics of the unperturbed case exhibits the ballistic spread instead of the localization such as,

$$m_2(t) \sim t^2. \quad (\text{B1})$$

Such a ballistic motion is suppressed and changes into other kind of motion by introducing the dynamically oscillating part ($W \neq 0$, $\epsilon \neq 0$).

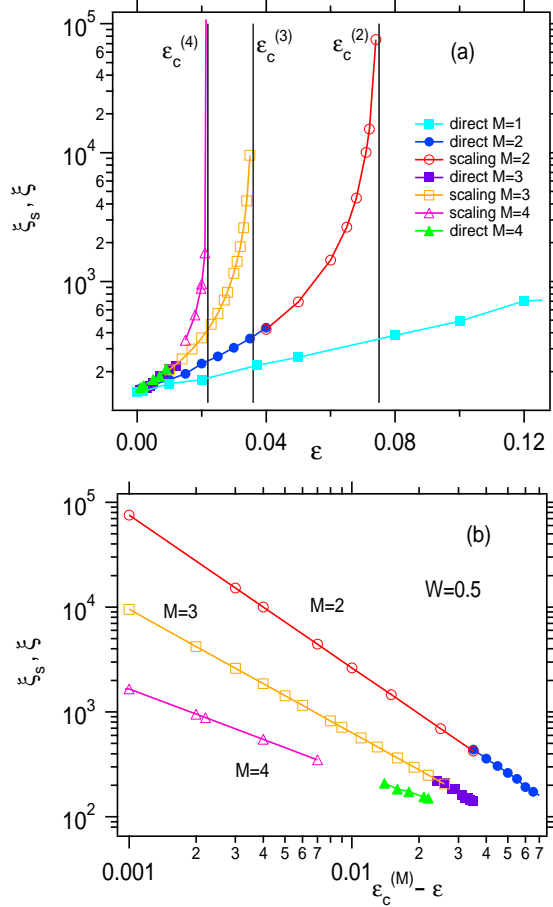


FIG. 13: (Color online) (a) The localization length $\xi(\epsilon)$, $\xi_s(\epsilon)$ as a function of ϵ for perturbed AM ($M = 1, 2, 3, 4$) with $W = 0.5$. The filled symbols denote the numerical data obtained by $\xi(\epsilon) = \sqrt{m_2(t \rightarrow \infty)}$ in the long-time limit. The open symbols indicate the localization length $\xi_s(\epsilon)$ obtained by the OPST in the critical region. Note that the vertical axis is in the logarithmic scale. (b) $\xi_n(\epsilon)$ and $\xi_s(\epsilon)$ as a function of $\epsilon_c^{(M)} - \epsilon$.

Figure 14 shows the time-dependence of the MSD with changing ϵ and M as the perturbation is applied. As shown in the Fig.14 (a), the MSD changes from $m_2(t) \sim t^2$ to $m_2(t) \sim t^1$ when the perturbation term on. Similarly, as shown in the Fig.14(b), there is no subdiffusion even in the cases of $M = 1 \sim 5$, and it behaves normal diffusion, $m_2(t) \simeq Dt$ for $t \gg 1$, where D is the diffusion coefficient.

The (ϵW) -dependence of the diffusion coefficient D is shown in the Fig.15. It can be seen that when the parameter ϵW becomes larger than $(\epsilon W)^* = 0.78$, the D gradually approaches a certain value. It follows that even in the monochromatically perturbed AM, there is no localization and normal diffusion is achieved. These phenomena can also be interpreted based on the Maryland transform. For $\epsilon W > 0$, it becomes diffusive by the hopping term including the disorder. When the W farther

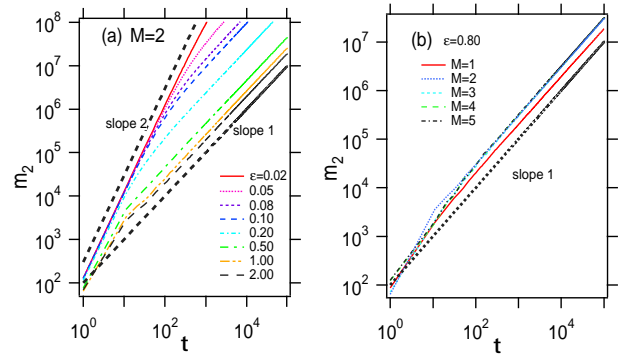


FIG. 14: (Color online) The double-logarithmic plots of $m_2(t)$ as a function of t for different values of ϵ in the polychromatically perturbed ballistic model $W = 1$. (a) $M = 2$ with various values of ϵ , and (b) $M = 1 \sim 5$ with $\epsilon = 0.8$. Black dotted lines show $m_2(t) \propto t^2$ and $m_2(t) \propto t^1$ for reference.

increases, the diffusion is suppressed due to the disorder and the diffusion coefficient is reduced. Even if W is further increased, the disorder effect seems to be saturated because the off-diagonal term is also tangent-type.

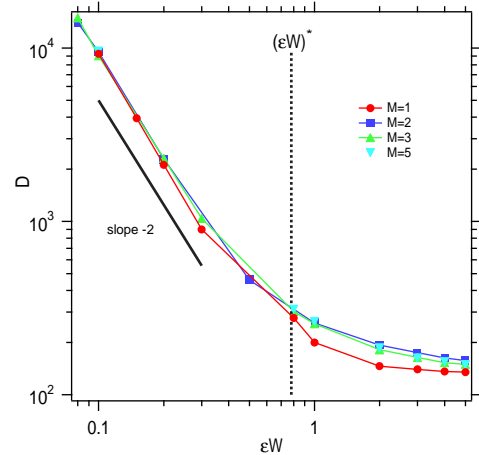


FIG. 15: (Color online) The diffusion coefficient D of the quantum diffusion as a function of ϵW in the polychromatically perturbed ballistic model ($M = 1 \sim 5$). Note that the axes are in the logarithmic scale. $(\epsilon W)^* = 0.78$ is shown by black dotted lines for reference.

Acknowledgments

This work is partly supported by Japanese people's tax via JPSJ KAKENHI 15H03701, and the authors would like to acknowledge them. They are also very grateful to Dr. T.Tsujii and Koike memorial house for using the facilities during this study.

-
- [1] J.Chabe, G.Lemarie, B.Gremaud, D.Delande, and P.Szrftgiser, Phys. Rev. Lett. **101**, 255702(2008).
- [2] J. Wang and A. M. Garcia-Garcia, Phys. Rev. E **79**, 036206(2009).
- [3] G. Lemarie, H.Lignier, D.Delande, P.Szrftgiser, and J.-C.Garrau, Phys. Rev. Lett. **105**, 090601(2010).
- [4] C. Tian, A. Altland, and M. Garst, Phys. Rev. Lett. **107**, 074101(2011).
- [5] M.Lopez, J.F.Clement, P.Szrftgiser, J.C.Garrau, and D.Delande, Phys. Rev. Lett. **108**, 095701(2012).
- [6] M. Lopez, J.-F. Clement, G. Lemarie, D. Delande, P. Szrftgiser, and J. C. Garreau, New J. Phys. **15**, 065013(2013).
- [7] K.Ishii, Prog. Theor. Phys. Suppl. **53**, 77(1973).
- [8] L.M.Lifshiz, S.A.Gredeskul and L.A.Pastur, *Introduction to the theory of Disordered Systems*, (Wiley, New York,1988).
- [9] H.S. Yamada and K.S. Ikeda, arXiv:1911.02189 [cond-mat.dist-nn] (2019).
- [10] H.S. Yamada, F. Matsui and K.S. Ikeda, Phys. Rev. E **92**, 062908(2015).
- [11] H.S. Yamada, F. Matsui and K.S. Ikeda, Phys. Rev. E **97**, 012210(2018).
- [12] S. Fishman, D.R.Grempel, R.E.Prange, Phys. Rev. Lett. **49**, 509 (1982); D.R. Grempel, R.E. Prange and S. Fishman, Phys. Rev. A **29**, 1639(1984); R.E. Prange, D.R. Grempel, and S. Fishman, Phys. Rev. B **29**, 6500-6512(1984).
- [13] P. Markos, Acta Phys. Slovaca **56**, 561(2006).
- [14] Antonio M. Garca-Garcia and Emilio Cuevas, Phys. Rev. B **75**,174203(2007).
- [15] Yoshiki Ueoka, and Keith Slevin, J. Phys. Soc. Jpn. **83**, 084711(2014).
- [16] E. Tarquini, G. Biroli, and M. Tarzia, Phys. Rev. B **95**, 094204(2017).
- [17] H.S.Yamada and K.S.Ikeda, Eur. Phys. J. B **85**,195(2012); *ibid* **87**, 208(2014).
- [18] H.Yamada and K.S.Ikeda, Phys. Rev. E **59**, 5214(1999); *ibid*, **65**, 046211(2002).
- [19] H.Yamada and K.S.Ikeda, Phys. Rev. E **65**, 046211(2002).
- [20] H.S. Yamada and K.S. Ikeda, in preparation.
- [21] This is also true for the Anderson transition in the three-dimensional disordered system. Mathematically, there is a proof of the existence of low-energy eigenstates characterized by the localization length even in the higher-dimensional random systems. There is something interesting about how the localization length connect to that numerically obtained by the finite-size scaling?